Chapter

Predicting the Behaviour of Oscillators Using Describing Functions

Owen Casha

Abstract

This chapter explores the application of describing functions in predicting the behaviour of non-linear oscillators. Describing functions offer an approximate method that simplifies the analysis of complex, non-linear systems by linearising their frequency response characteristics. This chapter delves into the theoretical foundations of describing functions and their practical use in predicting limit cycles in oscillators, highlighting their capacity to estimate the amplitude and the frequency of the oscillations. Through analytical derivations and case studies, this work demonstrates how describing functions bridge the gap between rigorous non-linear analysis and practical engineering approximations. The limitations, accuracy considerations, and alternative techniques are also discussed, providing a comprehensive understanding of when and how to effectively use describing functions in oscillator analysis and design. The discussion is supported by a literature survey on the use of describing functions in oscillator design and analysis and its relevance to automatic amplitude control mechanisms and the minimisation of AM-to-PM noise conversion.

Keywords: describing functions, non-linear oscillators, limit cycles, automatic amplitude control, AM-to-PM conversion

1. Introduction

The expanding market for communication systems has led to a rising demand for diverse radio frequency (RF) transceivers, driving significant growth in research and development in this field. A key requirement for RF transceiver applications is an integrated local oscillator (LO) that meets specific design criteria, including low phase noise, minimal power consumption, cost-effectiveness, high circuit integration with a small silicon footprint, and a wide tuning range [1]. Predicting the behaviour of a LO is a fundamental component in carrying out its analysis, design and implementation. A practical oscillator is classified as a non-linear system since an ordinary linear differential equation or a transfer function cannot solely model it. An oscillator features intentional non-linear mechanisms that are included on purpose in its feedback loop to provide sustained and predictable oscillations. In addition, an oscillator may also have secondary inherent non-linearities due to both active components and tuning components used in the circuitry. Secondary non-linearities are often

undesirable and lead to issues such as amplitude-to-phase (AM-to-PM) noise conversion [2].

A non-linear system can exhibit different modes of equilibrium, some of which are stable and others which are not, depend on the triggering input and initial conditions. Furthermore, a non-linear system such as an oscillator may, under certain conditions, exhibit oscillatory behaviour with a constant amplitude and frequency. This behaviour is called a limit cycle. Limit cycles can be stable or unstable. A stable limit cycle can be triggered even if the input and circuit conditions are not exactly equal to the specific values that correspond to the limit cycle. On the other hand, in the case of an unstable limit cycle, to stimulate it, conditions of the triggering input and circuitry must be perfectly equal to some specific values that depend on the governing equations. A small deviation from these values will fail to trigger the limit cycle. Thus, one must design an oscillator that features a robust and stable limit cycle across a range of process, supply voltage and temperature variations [3].

As yet there is no general or unified tool for analysing non-linear systems of any type. There are several methods, each of which could be applied to a specific type of non-linear system. The phase-plane method is a graphical method, which is accurate but is restricted to second-order systems [4]. The Lyapunov method is the most complete that, in principle, could be used to analyse the stability of any system. However, it involves determining the so-called Lyapunov function for each system to be analysed, and this is not always an easy task [4]. The describing function method (DFM) approximates non-linear elements in a system by an equivalent linear one. While this introduces some errors, it makes the analysis simpler. It handles the problem from a frequency response point of view. The good features of the DFM are that it is a relatively simple technique, it is valid for any system order and it provides information about the system's stability properties, including the presence of limit cycles. Nonetheless, it is based on an approximation: it applies only to non-linear systems whose linear components have low-pass or band-pass filtering properties (thus attenuating high-frequency components) and gives no information about the transient response [4]. Since the DFM provides information on the presence of limit cycles and oscillators include passive networks that exhibit low-pass or band-pass filtering properties, this method is convenient and applicable in predicting the behaviour of oscillators.

The DFM is intuitive and computationally efficient, making it suitable for a preliminary design and insight into oscillation conditions. However, the DFM assumes sinusoidal inputs and neglects higher harmonics, which limits accuracy, especially for strongly non-linear or discontinuous systems. Another technique reported in the literature is called harmonic balance, which, in contrast, includes multiple harmonics in its solution by expressing the oscillator behaviour as a truncated Fourier series and solving for balance in the frequency domain. This method captures non-linearities more accurately than the DFM and can model periodic solutions with greater fidelity. However, it requires solving a non-linear algebraic system, making it computationally heavier than the DFM and less suitable for systems with broadband or chaotic behaviour [5]. Another approach is the numerical continuation method, which traces the evolution of solutions (including steady-state and periodic orbits) as the parameters change, providing powerful insights into bifurcations and stability. Unlike the DFM and harmonic balance, numerical continuation does not rely on simplifying assumptions about the signal shape, making it highly accurate. It can handle complex, multistable, and discontinuous systems. However, it demands significant computational resources and careful initialisation, often requiring prior knowledge of a solution

branch [6]. In summary, the DFM is fast and useful for basic predictions, harmonic balance improves accuracy with moderate complexity, and numerical continuation offers high fidelity at the cost of computational effort. The choice depends on the oscillator's non-linearity, required accuracy, and available resources.

In addition to the introductory section, this chapter is divided as follows. **Section 2** presents a concise but informative literature review of various publications which focused on the application of the DFM to analyse and predict the behaviour of oscillators. **Section 3** presents the theoretical background of the DFM. The discussion is aided by applying this approach to analyse the Van der Pol oscillator [4], which is classical example of a non-linear system exhibiting a limit cycle. This section delves into the theoretical foundations of describing functions and their practical use in predicting limit cycles in oscillators, highlighting their capacity to estimate the amplitude and frequency of their oscillations. **Section 4** provides analytical derivations of two oscillator case studies, showing how describing functions bridge the gap between a rigorous non-linear analysis and practical engineering approximations. **Section 5** presents and discusses the relevance of describing functions to automatic amplitude control mechanisms and the minimisation of AM-to-PM noise conversion. Finally, **Section 6** provides some concluding remarks and highlights the main achievements and the limitations of this work while proposing potential future research avenues that may be considered in the coming years.

2. Literature review

2.1 Historical perspective

The describing function (DF) analysis is a classical method for handling non-linear systems and predicting oscillations and limit cycles. Its roots trace back to the 1930s with the work of Krylov and Bogolyubov, who developed a harmonic linearisation approach to approximate non-linear oscillations [7]. The technique was later extended and formalised in the late 1940s and 1950s. In the west, Tustin (UK) and Kochenburger (USA) were early pioneers. The work presented in Ref. [8] applied frequency-response methods to on-off contactor servomechanisms, effectively introducing the DFM to control engineering. In parallel, Soviet researchers like Goldfarb built on Krylov-Bogolyubov's work and made the DFM a standard analysis tool in the USSR by the late 1940s [9]. These developments ran in parallel across countries, with similar concepts emerging in Germany (Oppelt) and France (Dutilh) as well [9]. By the 1960s, the DFM was well established. The work presented in Refs. [10–12] documented the method and broadened its scope to multiple-input systems [12]. The technique's use expanded beyond its control theory origins to oscillator design in electronics. The work [13] showed that describing-function techniques were successfully applied to thermally self-excited mechanical oscillators and were able to predict amplitude and frequency in accurate agreement with experimental investigation [13]. Throughout the following decades, the DFM continued to be used and refined in different fields. In electrical engineering, DFM became an important tool to analyse sinusoidal oscillator start-up and amplitude stabilisation, complementing the linear Barkhausen criterion [11, 13]. Other research also introduced extensions like two-port describing functions to model active devices in oscillators and higher-order describing functions for considering multiple harmonics [12]. These extended forms paved the way for applying DF analysis to modern RF oscillators and systems with more complex non-linearities. Interest in the DF approach also saw a revival in specialised areas,

including power electronics circuits such as the self-resonant inverter oscillators, robotics, and biological oscillators [14].

2.2 Strengths and limitations of describing functions

2.2.1 Strengths and advantages

The DF analysis offers several key advantages when dealing with non-linear oscillators. Foremost, it greatly simplifies non-linear system analysis by reducing a non-linear element to an amplitude-dependent transfer function. This quasi-linearisation approach retains essential non-linear behaviour (such as amplitude saturation) while allowing the use of linear analysis techniques, including the Nyquist or the Routh criterion [4, 14]. The DFM can predict the existence and characteristics of limit cycles in a feedback system by treating the non-linear block as if it were a linear gain and phase block that depends on signal amplitude [10]. This enables one to determine the steady-state oscillation amplitude and frequency without the need to solve the full non-linear differential equations. The DF provides a way to find the oscillation amplitude and frequency by solving an algebraic condition at certain amplitude rather than requiring a time-domain simulation [10]. In an operational transconductance amplifier (OTA)-based RC oscillator study, the DFM accurately predicted the stable oscillation amplitude, and the results were confirmed using MATLAB and PSpice simulations [10].

Such agreement confirms that the DF gives meaningful quantitative insight into oscillator behaviour. Another strength is the physical insight it provides into non-linear oscillator dynamics, such as amplitude stabilisation. Traditional linear oscillator theory, such as Barkhausen's criterion, explains how an oscillation starts but not how it limits in amplitude. The describing function fills this gap by modelling how an amplifier's effective gain is effectively adapted to stabilise the amplitude [11]. This explains that a non-linear oscillator requires a form of gain compression (or expansion) to achieve a steady-state response [12]. Indeed, the describing function-based method enhances the oscillator design by complementing Barkhausen's criterion with amplitude control analysis [12]. The method yields intuitive graphical results in the complex plane, where the intersection of the Nyquist plot with the inverse describing function makes it easier to visualise how a limit cycle is sustained [15].

Furthermore, the DF approach is quite generic and widely applicable. It does not depend on the physical nature of the system—only on the presence of a non-linear feedback loop. It has been applied successfully to electronic amplifiers, mechanical structures, and even abstract models, indicating the robustness of the approach [13]. As long as the system can be seen as a linear element in feedback with a single non-linearity, the same DF procedure can predict the oscillation conditions. This cross-domain flexibility implies that such a technique can be applied to both an analogue transistor oscillator and a thermo-mechanical oscillator. The main advantage of the DFM is that it allows the inclusion of the non-linear behaviour of a system while maintaining the simplicity often associated with linear system analysis [14]. It provides a straightforward way to estimate the oscillation amplitude, frequency, and even distortion level [14], which would otherwise require a much more complex analysis.

2.2.2 Limitations and caveats

Despite its usefulness, the DFM has important limitations. It relies on several restrictive assumptions about the system, which, if violated, can cause large errors or

analysis failure. The classical DF approach assumes only a single time-invariant memoryless non-linear element exists in the loop and that the oscillation is dominated by its fundamental harmonic [10]. This means the method works best when the non-linearity is a simple static function (such as saturation, cubic gain or dead-zone) and when the oscillator's waveform is nearly sinusoidal. Under those conditions, one can ignore higher harmonics and treat the non-linear block like an effective gain at the fundamental frequency. An additional common assumption is that the non-linearity is odd-symmetric, so it does not produce even-harmonic or d.c. components [10]. While not strictly required, this condition simplifies the analysis by ensuring that the output has no bias and the fundamental frequency is the dominant term. If the system deviates from these assumptions, the DF predictions lose their validity.

One major limitation is the accuracy loss in systems with strong non-linearities or non-sinusoidal oscillations. The DF uses only the first harmonic of the non-linear response. Thus, if the actual oscillator waveform contains substantially higher harmonics, the DF is a crude approximation. In cases where the linear part of the system does not filter out higher order harmonics, such as in relaxation oscillators [16] or digital-like ring oscillators [17], the fundamental approximation breaks down. As a result, the DFM may fail when the higher harmonics significantly influence the behaviour [4]. For bang-bang control systems, the method might predict a limit cycle that is very different from reality or miss an existing oscillation [4]. Similarly, a Schmitt-trigger oscillator, which includes a comparator with hysteresis driving an integrator, produces a highly distorted square or triangle waveform. A basic DF analysis of such a system is likely to be inaccurate or even predict no oscillation since the method cannot capture the piecewise-linear jumps. The output of a Schmitt-trigger relaxation oscillator violates the single-frequency assumption, illustrating where DF analysis is inadequate.

Another limitation is that the DFM requires single-valued non-linearities with no hysteresis or memory. If the non-linearity has memory (such as rate-dependent hysteresis), the simple DFM is not directly applicable [10]. In such cases, more complicated extensions or entirely different methods are needed. Even for static non-linearities, the describing function provides no guarantee of finding all the possible oscillatory solutions—it might find one stable limit cycle, but a system could have multiple limit cycles or complex dynamics exhibiting sub-harmonics or quasi-periodicity. These cannot be predicted by a first-harmonic analysis. Highly non-linear or borderline chaotic systems are essentially beyond the scope of the standard DF approach because they violate the underlying assumption of one dominant frequency. Additionally, the DFM typically gives no information or insight about the transient behaviour or how the oscillation builds up; it only predicts the steady-state amplitude and frequency if a limit cycle exists. It is also worth noting that the DFM, being approximate, sometimes predicts an oscillation that in reality does not occur or misses an existing oscillation. For example, one study applied a two-port describing function to a transistor Colpitts oscillator and found some deviation between the DF-based design predictions and the measured oscillation, which was attributed to modelling errors [12].

This highlights that the DF results are only as good as the model of the non-linear element. If the actual device behaviour differs, such as in the case it has a frequency-dependent non-linearity or significant parasitic dynamics, the DF analysis can be off target. Finally, while graphical DF and Nyquist constructions are convenient, they can become cumbersome for very complex systems, and they do not readily extend to cases with multiple independent non-linearities in the loop. Despite these caveats,

many limitations of describing functions are well understood, and there are extensions to mitigate them. For instance, higher-order sinusoidal input describing functions (HOSIDF) may be included to account for second or third harmonics if needed [18]. There are also describing function matrices for multiple-input multiple-output non-linearities and the so-called X-parameters in microwave engineering, which generalise the DF concept to multi-tone steady-state behaviour [12]. These advanced techniques can handle some cases of strong nonlinearity at the cost of more complexity. In summary, the strength of the DF method is in analysing well-behaved single-frequency oscillations with mild non-linearities. When used with awareness of its assumptions and possibly augmented by higher-harmonic corrections, it remains a powerful tool. But for systems that lie outside its valid assumptions, such as those featuring very sharp non-linearities, multi-frequency oscillations, or chaotic regimes, one must resort to time-domain simulation or more exact analytic methods instead of relying on the DFM alone.

2.3 Application in specific oscillator types

2.3.1 Sinusoidal and relaxation electronic oscillators

In electronic oscillator design, DF is often used to design and predict the performance of sinusoidal oscillators that incorporate an amplitude-limiting non-linearity. A classic example is the Wien bridge oscillator. This oscillator uses an amplifier with an automatically adjusting gain (implemented as a small incandescent lamp or a pair of diodes in the feedback path) to stabilise the output amplitude. The describing function of the non-linear lamp or the diode network can be used to find the steady-state oscillation amplitude: essentially, one finds the output voltage at which the non-linear element's effective gain causes the loop gain to be exactly unity. The DFM predicts, for example, the amplitude at which an op-amp Wien bridge will level off given the diode's transfer characteristic curve, and it can estimate the distortion based on how non-sinusoidal the waveform becomes when the limiter engages [14].

Another common application is in LC and RC oscillators using active devices like transistors or operational amplifiers with non-linear gain characteristics [14]. The work presented in Ref. [12] applied a two-port DFM to a BJT Colpitts oscillator design. A describing function for the transistor was derived by modelling it as non-linear two-port admittance and solved for the oscillation in the frequency domain. The design achieved oscillation in the MHz range, and Meszaros et al. [12] reported good agreement between the DF-based analytical predictions and SPICE circuit simulations, as well as reasonable correspondence with experimental measurements [12]. Minor discrepancies were noted, likely due to the transistor model limitations, but these were to be addressed with refined modelling in a follow-up work [12]. The work in Ref. [12] demonstrates how DFM can be used in practical RF oscillator design. By capturing the amplitude-dependent negative resistance of the active device, one can predict the steady-state oscillation amplitude and frequency without a full time-domain simulation. DF analysis has also been used for ring oscillators and relaxation oscillators, although these push the method to its limits. A ring oscillator, which consists of a chain of inverters and produces a square wave, violates the pure single-frequency assumption, yet the work in Ref. [15] has adapted the DF analysis to this special case. The work in Ref. [15] showed that even for a ring oscillator, one can apply a quasi-linear describing function approach by accounting for the phase shift of each inverter stage and the saturation non-linearity of its output, although higher harmonics are

significant. In such cases, the describing function is used to estimate the fundamental oscillation frequency and ensure start-up while acknowledging that the waveform is far from sinusoidal. Relaxation oscillators, including multivibrators or the Schmitt-trigger and integrator configuration, are similarly challenging. The DFM can predict the existence of a limit cycle in a Schmitt-trigger oscillator by modelling the hysteresis as an effective non-linear element; indeed, this topology has been used as an example in DF analysis discussions. However, because the oscillation is a highly non-sinusoidal sawtooth or square waveform, a basic DF analysis might give only a rough estimate of frequency and an overly optimistic assumption of a sine-wave output. In practice, one may use DF in relaxation oscillator design simply to verify that a limit cycle will occur under certain bias conditions and then use exact calculations or simulations for the precise waveform and period.

Another important category is automatic gain control (AGC) oscillators and amplitude-regulated oscillators. Many RF and analogue oscillators include an AGC loop or a non-linear gain element to control amplitude, such as a field-effect transistor operated in its non-linear region or a gain-control element driven by a rectified output. The DFM is extremely useful here: it can model the AGC's effect and predict the final amplitude. The work in Ref. [11] emphasises that relying on Barkhausen's criterion alone is inadequate, and one must incorporate non-linear gain compression to truly design an oscillator. DF, coupled with the Routh-Hurwitz stability analysis, forms a systematic method to design oscillators beyond the small-signal threshold point [11]. For instance, in operational amplifier-based oscillators (such as the Wien bridge or phase-shift oscillator), Barkhausen gives the frequency of oscillation, but the DF analysis yields the amplitude at which the non-linearity (or an explicit limiter) of the operational amplifier balances the loop gain to unity [11].

2.3.2 Mechanical and MEMS oscillators

DFM has also been applied to oscillators outside the purely electrical realm, including macroscopic mechanical oscillators and microelectromechanical systems (MEMS) oscillators. The underlying principle—a non-linear feedback loop reaching a self-sustained oscillation—is common to many physical systems, so the DFM can often be ported from circuits to mechanics with appropriate modelling. One of the earliest cross-domain applications was thermally self-excited mechanical oscillators. The work reported in Ref. [13] used DF analysis to predict the behaviour of a pendulum oscillating due to the periodic heating and cooling of a wire, which is a form of self-excited vibration. In Ref. [13], the non-linear relationship between the wire's temperature (and length) and the oscillation amplitude was modelled, and then treated the mechanical system's dynamics as the linear part of a feedback loop [13]. This work showed the broad utility of DF techniques to explain phenomena behind a thermal swing pendulum or a hammock oscillator driven by thermal expansion cycles [13]. While the analysis was approximate, it captured the essential self-limiting nature of the oscillation. The work in Ref. [13] also highlighted that the same DF approach could apply to very different physical energy sources, as long as one can identify a non-linear restoring force or gain element. Beyond thermal oscillators, describing functions have been used to study other mechanical limit cycles. For example, systems with dry friction or backlash can exhibit sustained oscillations (stick-slip motion), and DF analysis has been one of the tools to predict the amplitude of limit cycles in such systems by approximating the friction force versus velocity as a non-linear function. Another application is vehicle or aircraft autopilot oscillations, often called hunting

oscillations. Even though these are electro-mechanical systems, classical analyses used DF to estimate limit cycle conditions when a control system had a saturating actuator or a dead zone.

In the context of MEMS oscillators, DF techniques are likewise applicable, although the literature is not as extensive as for electronic circuits. MEMS oscillators, such as vibrating microbeams or micromechanical resonators with an amplifying circuit, often include non-linear effects like amplitude-frequency coupling (Duffing stiffness) or electronic limiting for amplitude stabilisation [19]. DF analysis has been applied in the design of MEMS frequency sources and sensors. For instance, in the design of a silicon micromachined resonant accelerometer [20], an oscillation loop is formed to keep a micro-resonator vibrating, and an automatic amplitude control is used to stabilise the vibration. The describing function for the non-linear amplifier in the loop was derived to calculate the steady-state oscillation amplitude and ensure it stayed within safe limits [20]. This aided the design of the control electronics so that the MEMS resonator operates in a stable limit cycle rather than ringing up to destructive levels or decaying to zero. Similarly, in the study of coupled MEMS oscillators (for injection locking or synchronisation phenomena), simplified describing function models have been used to reduce the non-linear coupling force to an equivalent gain-phase element, which aid in predicting oscillations and phase locking behaviour without heavy computation [21]. These analyses remain somewhat qualitative, but they extend the intuition of describing functions. Another interesting application in the mechanical realm is in robotics and biomechanics. Limit-cycle oscillators appear in legged locomotion (robotic gait engines) and neuro-inspired oscillators (central pattern generators). Some researchers have employed describing function analysis to design rhythmic motion controllers—essentially treating the non-linear robot actuator dynamics as elements in an oscillator loop and using the DFM to ensure a stable limit cycle with desired amplitude [14]. Even for complex systems that can exhibit chaos, like a robot manipulator with non-linear feedback, the DFM has been used to identify periodic orbits and sometimes even to predict the onset of chaotic motion, even though for chaotic systems, other methods are more suitable [14].

3. Describing function method - theoretical background

The DFM is a widely used analytical tool in non-linear control, particularly for systems exhibiting periodic behaviour such as non-linear oscillators. This method approximates non-linear system dynamics by reducing the non-linearity to an equivalent gain and phase shift when subjected to sinusoidal inputs [4]. By characterising the non-linear element using a describing function, one can predict the conditions under which oscillations occur, offering an effective means of analysing self-sustained oscillators. In oscillator design, the DFM identifies the oscillation amplitude and the frequency by locating the intersection between the non-linear describing function and the linear system's frequency response. The method relies on the assumption that the system predominantly responds at the fundamental frequency, simplifying the analysis of complex non-linear interactions. This assumption, although approximate, is often sufficiently accurate for practical oscillator applications. The DFM enables the exploration of stability and performance trade-offs, providing insights into limit cycles and bifurcation phenomena. The method has limitations, such as reliance on accurate modelling of non-linearities and the inability to predict sub-harmonic or chaotic responses.

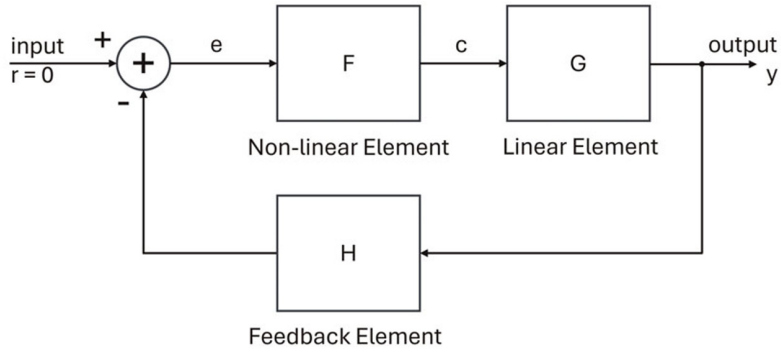

Figure 1.
Block diagram closed loop representation of a generic oscillator.

Figure 1 presents a block diagram representation of a generic oscillator with output y and input r which is set to zero. By means of the DFM, the non-linear element F can be represented by an approximate linear transfer function in terms of the frequency response F_D. Suppose that the input e to the non-linear element F is sinusoidal. The output of the non-linear element c is, in general, not sinusoidal but periodic with the same period as the input e, since the output c would be a complex wave which contains higher harmonics. This output $c(t)$ can be expressed in terms of its Fourier series:

$$c(t) = \frac{A_0}{2} + \sum_{k=1}^{\infty} (A_k \cos(k\omega t) + B_k \sin(k\omega t)) \tag{1}$$

$$A_k = \frac{1}{\pi} \int_0^{2\pi} c(t) \cos(k\omega t) d\omega t \tag{2}$$

$$B_k = \frac{1}{\pi} \int_0^{2\pi} c(t) \sin(k\omega t) d\omega t \tag{3}$$

where k is the harmonic number and ω is the angular frequency of the non-linear element input signal. In the describing function analysis, one assumes that only the fundamental harmonic component of the output $c(t)$ is significant. Such an assumption is often valid since the higher harmonics in the output of the non-linear element are often of smaller amplitude than those of the fundamental component. In addition, oscillators often include a linear element G that exhibits a low-pass or a band-pass frequency response, with the result that the higher harmonics are highly attenuated with respect to the fundamental harmonic component and so the oscillator output y can be considered as a pure sinusoidal signal, thus confirming the initial assumption that e is sinusoidal.

The describing function of the non-linear element is defined to be the ratio of the phasor representing the fundamental component of the output $c(t)$ to the phasor representing the input $e(t)$:

$$F_D(j\omega, M) = \frac{C_1 \angle \Phi_1}{M} \tag{4}$$

where C_1 is the amplitude of the fundamental component of the non-linear element's output, Φ_1 is the phase difference between the output's fundamental component and the input signal *e(t)* and M is the amplitude of the input signal which is assumed to be sinusoidal. Very often the non-linear elements in oscillators are skew symmetric or odd functions, such that A_0 is zero. Thus, the fundamental component of *c(t)* would not have any d.c. term and with reference to Eq. (4),

$$C_1 = \sqrt{A_1^2 + B_1^2} \tag{5}$$

$$\Phi_1 = \tan^{-1}\left(\frac{A_1}{B_1}\right) \tag{6}$$

It is thus clear that $F_D(j\omega, M)$ would be a complex quantity when Φ_1 is non-zero. If no energy-storage element is included in the non-linear element, then $F_D(j\omega, M)$ is only a function of the amplitude of the input of the element. This is called a static non-linearity. On the other hand, if an energy-storage element is included, then $F_D(j\omega, M)$ is a function of both the amplitude and frequency of the input. As a summary, since in the context of a non-linear oscillator, there is typically one non-linear element in the loop or various non-linearities that could be grouped as one component and the non-linear element is followed by either a low-pass or band-pass filtering network, one is justified in using the describing function analysis, where one replaces the non-linear block F by $F_D(j\omega, M)$. Thus, one may then apply the classical stability techniques based on the frequency response such as the Nyquist criterion or the Barkhausen criterion.

In order to explore and understand, how the DFM can be applied to analyse the behaviour of non-linear oscillators while identifying its limitations, a classical oscillator known as the Van der Pol oscillator, will be studied and evaluated. The Van der Pol oscillator is a non-linear system described by a second-order differential equation and was introduced by Dutch physicist Balthasar van der Pol in 1927, while working at Philips [4]. The Van der Pol oscillator is governed by Eq. (7):

$$\frac{d^2y}{dt^2} - \alpha\left(1 - y^2\right)\frac{dy}{dt} + y = 0 \tag{7}$$

where y is the output and α is the parameter that controls the non-linearity and the damping. Unlike simple harmonic oscillators, it includes a non-linear damping term (the coefficient of $\frac{dy}{dt}$) that allows for self-sustained oscillations. When y^2 is less than unity, the system is unstable and so y starts to increase due to a negative damping coefficient, while when y^2 is greater than unity, the system start losing energy due to a positive damping coefficient and y starts to decrease. Energy is added or dissipated depending on the system's state, stabilising oscillations at a limit cycle. Rearranging Eq. (7) as follows:

$$\frac{d^2y}{dt^2} - \alpha\frac{dy}{dt} + y = -\alpha y^2\frac{dy}{dt} = \alpha c(t) \tag{8}$$

where

$$c(t) = F(e(t)) = -y^2\frac{dy}{dt} \tag{9}$$

$$e(t) = r(t) - y(t) = -y(t) \tag{10}$$

allows to model the Van der Pol oscillator according to the generic model as shown in **Figure 2**. In this case, the feedback element is equal to unity.

Now as per the DFM, assuming $y(t)$ is a sinusoid with amplitude M:

$$y(t) = Msin(\omega t) \tag{11}$$

gives an expression for the output of the non-linear element $c(t)$:

$$c(t) = -(Msin(\omega t))^2 \frac{d(Msin(\omega t))}{dt} = -(Msin(\omega t))^2 M\omega cos(\omega t) \tag{12}$$

which can be simplified to:

$$c(t) = -\frac{M^3 \omega cos(\omega t)}{4} + \frac{M^3 \omega cos(3\omega t)}{4} \tag{13}$$

by using trigonometric identities. Eq. (13) shows that $c(t)$ is composed of a fundamental frequency equal to that of $y(t)$ and a third harmonic of the same magnitude as the fundamental of $c(t)$. Since the linear element is a second order low-pass filter, the third harmonic of $c(t)$ will be ignored since it will be filtered out. Writing the fundamental of $c(t)$ as:

$$C_1(t) = -\frac{M^2}{4} M\omega \, cos\,(\omega t) = -\frac{M^2}{4}\,\frac{dy}{dt} \tag{14}$$

the describing function of the non-linear element is obtained as follows:

$$F_D(j\omega, M) = \frac{j\omega M^2}{4} \tag{15}$$

such that the characteristic equation of the Van der Pol oscillator can be expressed as:

$$1 + \frac{\alpha}{(j\omega)^2 - \alpha(j\omega) + 1}\,\frac{j\omega M^2}{4} = 0 \tag{16}$$

Replacing the non-linear element in **Figure 2** by the describing function given in Eq. (15), one obtains the equivalent linear closed loop model of the oscillator, shown in **Figure 3**.

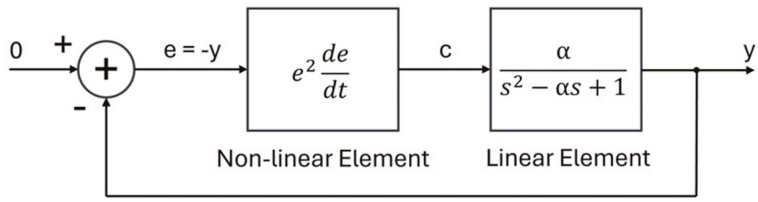

Figure 2.
Non-linear closed loop model of the Van der Pol oscillator.

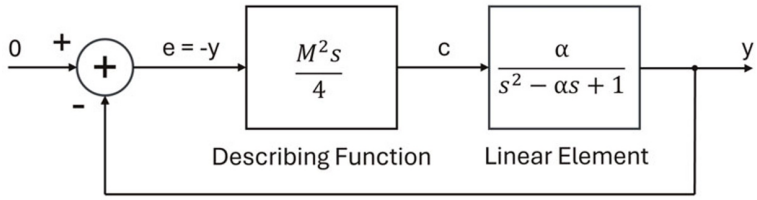

Figure 3.
Equivalent linear s-domain model of the Van der Pol oscillator.

By rationalising Eq. (16), one can express it as a real component:

$$\frac{M^2\alpha^2\omega^2}{(1-\omega^2)^2 + (\alpha\omega)^2} = 4 \tag{17}$$

and an imaginary component:

$$\frac{M^2\alpha(j\omega)(1-\omega^2)}{(1-\omega^2)^2 + (\alpha\omega)^2} = 0 \tag{18}$$

From Eq. (18), one obtains the oscillation angular frequency ω of 1 rad/s, while the oscillation amplitude M of 2 is obtained by substituting $\omega = 1\, rad/s$ in Eq. (17). Eq. (18) provides also another solution ($\omega = 0\, rad/s$), but this is a trivial solution. This result is confirmed by numerically integrating Eq. (7) for a value of $\alpha = 0.1$ and presented in **Figure 4**, where the simulated transient behaviour and the phase portrait of the non-linear oscillator are provided together with the single-sided amplitude spectrum of $y(t)$.

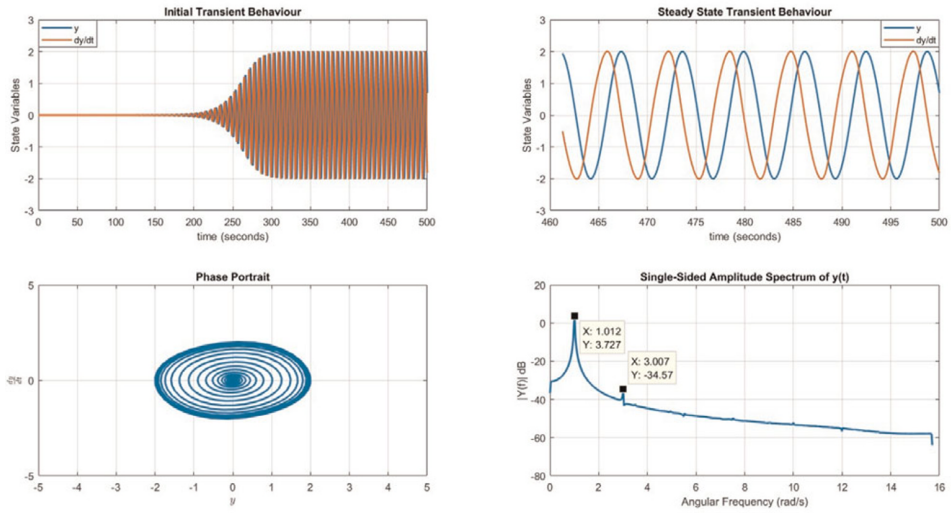

Figure 4.
Simulation results of the Van der Pol oscillator for $\alpha = 0.1$.

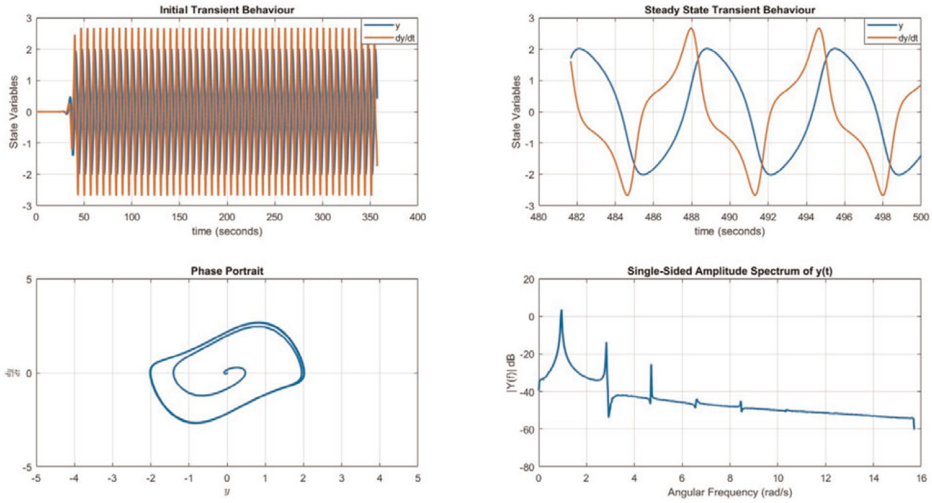

Figure 5.
Simulation results of the Van der Pol oscillator for $\alpha = 1$.

For a low value of α, the DFM is able to predict the behaviour of the non-linear oscillator in terms of amplitude and fundamental oscillation frequency, where the output $y(t)$ is almost purely sinusoidal since the third harmonic is much less than the fundamental (around 38 dB less). The gain frequency response $|G|$ of the linear element is given by Eq. (19):

$$|G| = \frac{\alpha}{\sqrt{(1-\omega^2)^2 + (\alpha\omega)^2}} \tag{19}$$

Eq. (19) shows that when ω is 1 rad/s (fundamental oscillator frequency), $|G|$ is always unity, while the value of $|G|$ at the third harmonic increases with the value of α. This means that in the Van der Pol oscillator, when one increases the value of α, the filtering of the harmonics is less effective, while the gain at the fundamental oscillator frequency remains the same. Thus, the assumption that linear element filters out the harmonics of the output $y(t)$ is less valid when α is increased. This is clearly shown for the simulation of the oscillator when $\alpha = 1$, whose results are presented in **Figure 5**, where the transient behaviour is more non-linear and the oscillator reaches the limit cycle in a shorter time. This shows that in non-linear oscillators, where the filtering action of the linear element is not effective, while the DFM still provides a correct value for the fundamental frequency and amplitude, the accuracy by which the DFM predicts the oscillator behaviour in terms of the total harmonic distortion starts to degrade.

4. Applying the DFM to practical oscillators

This section presents analytical derivations of two oscillator case studies, showing how the DFM can be applied to practical oscillators such as the differential negative resistance oscillator [22, 23] and the Colpitts oscillator [23, 24], to predict their oscillation frequency and amplitude.

4.1 Differential negative resistance oscillator

A circuit that is commonly used in LC tank oscillator designs is shown in **Figure 6** [1]. It uses an NMOS cross-coupled differential pair (M_1 and M_2) to synthesise the negative resistance required to achieve sustained oscillations [1, 22]. Since the outputs of the oscillator ($V_{OUT}+$ and $V_{OUT}-$) are in antiphase and the sources of the transistors are at a small signal differential ground, then the impedance looking down into the drain of M_1 can be shown to be equal to $-1/g_{m1}$, where g_{m1} is the transconductance of M_1.

Thus, to ensure constant amplitude oscillations, this negative resistance must be at least equal to the parasitic resistance of the LC tank connected to M_1. If g_m is too low, any oscillations will decrease in amplitude, while if it is too high, any oscillations will grow exponentially. To achieve constant amplitude oscillations with this oscillator topology, the non-linearity of the transistors is exploited [1, 22]. As the oscillation amplitude increases, the effective g_m of the active devices decreases due to the devices entering the triode region for part of the oscillation period. To ensure the start-up of the oscillator, the transconductance is chosen to produce a start-up gain greater than unity. Then, any initial perturbation grows exponentially, decreasing g_m, until a stable amplitude is reached. It is important to note that this oscillator has two modes of operation. The first mode is referred to as the current-limited regime of operation, in which the tank voltage amplitude is solely determined by the tail-current source I_{BIAS} and the LC tank equivalent resistance. When the amplitude of the tank voltage approaches a voltage greater than the supply V_{DD}, the NMOS transistors enter the linear region at the peaks of the voltage, and so the tank voltage amplitude does not significantly increase beyond that voltage since it is clipped at the source voltage of the NMOS transistors (M_1 and M_2). For the period that the NMOS transistors enter the linear region, they no longer present a negative resistance to the LC tank; thus, the phase noise response is degraded. It is then said that the oscillator has entered the

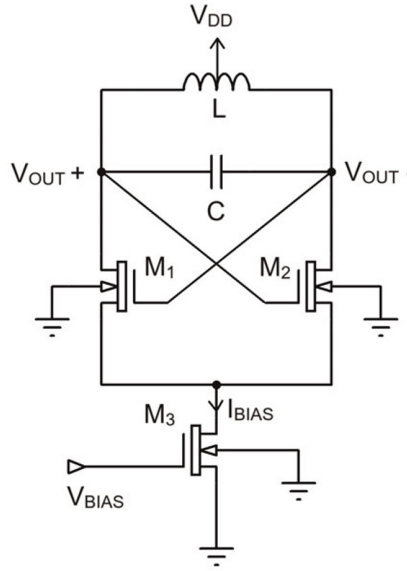

Figure 6.
NMOS-based differential negative resistance LC tank oscillator.

voltage-limited regime of operation. Note also that the tail NMOS transistor M_3 may spend most of its time in the linear region so the tail current does not stay constant but is dependent on the voltage across this NMOS transistor.

This oscillator can be represented using the non-linear closed-loop model given in **Figure 7**, which consists of a non-linear active element, an inversion unity gain that models the inverting nature of the active device, and an LC tank passive equivalent linear element circuit, where C is the capacitance, L is the inductance and R is the total equivalent loss of the tank circuit. The non-linear element is a saturation non-linearity, which is used to model the behaviour of the active device.

For small input signals, the output of the saturation non-linear element is proportional to the input, while for large input signals, the output is constant at the maximum possible output value $\frac{I_{BIAS}}{2}$. Thus for a sinusoidal input given by Eq. (20), the output waveform i_{OUT} becomes as shown in **Figure 8**, where M is the single-ended oscillation amplitude and ω is the angular oscillation frequency.

$$v_{OUT}(t) = -Msin(\omega t) \tag{20}$$

Since the saturation non-linear element is an odd non-linearity, the fundamental Fourier series coefficient A_1 can be shown to be equal to 0 using Eq. (2), while the fundamental Fourier series coefficient B_1 can be computed using Eq. (3). Given the symmetry of the waveform i_{OUT}, B_1 can be expressed as follows:

$$B_1 = \frac{4}{\pi}\int_0^{\frac{\pi}{2}} i_{OUT}(t)\sin(\omega t)d\omega t \tag{21}$$

$$B_1 = \frac{4}{\pi}\int_0^{\omega t_1} g_m M\sin(\omega t)\sin(\omega t)d\omega t + \frac{4}{\pi}\int_{\omega t_1}^{\frac{\pi}{2}} \frac{I_{BIAS}}{2}\sin(\omega t)d\omega t \tag{22}$$

By using Eq. (20) and equating it to $\frac{-I_{BIAS}}{2g_m}$, one may express t_1 as per Eq. (23):

$$t_1 = \frac{\arcsin\left(\frac{I_{BIAS}}{2g_m M}\right)}{\omega} \tag{23}$$

such that

$$B_1 = \frac{2g_m M}{\pi}\left(\arcsin\left(\frac{I_{BIAS}}{2g_m M}\right) + \frac{I_{BIAS}}{2g_m M}\sqrt{1-\left(\frac{I_{BIAS}}{2g_m M}\right)^2}\right) \tag{24}$$

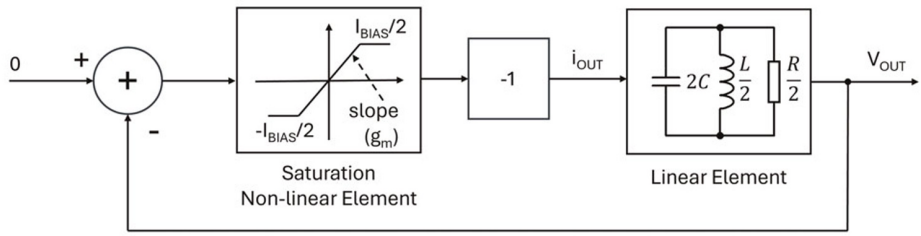

Figure 7.
Single-ended non-linear closed-loop model of the differential negative resistance oscillator.

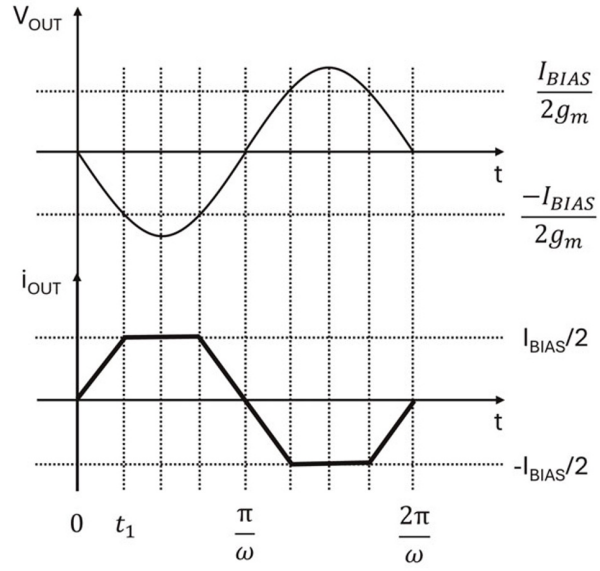

Figure 8.
Input and output waveforms for the saturation non-linear element.

By using Eq. (4), one can show that the static describing function $F_D(M)$ for the saturation non-linearity is given by:

$$F_D(M) = \frac{2g_m}{\pi}\left(\arcsin\left(\frac{I_{BIAS}}{2g_m M}\right) + \frac{I_{BIAS}}{2g_m M}\sqrt{1-\left(\frac{I_{BIAS}}{2g_m M}\right)^2}\right)\angle 0^\circ \tag{25}$$

For a large value of g_m, Eq. (25) can be simplified as follows:

$$F_D(M) = \frac{i_{OUT}}{-v_{OUT}} = \frac{2I_{BIAS}}{\pi M}\angle 0^\circ \tag{26}$$

The transfer function of the linear element $G(j\omega)$ is given by:

$$G(j\omega) = \frac{v_{OUT}}{i_{OUT}} = \frac{\frac{j\omega L}{2}}{(j\omega)^2 LC + \frac{j\omega L}{R} + 1} \tag{27}$$

which can be obtained from the total parallel impedance of the three passive components. By using the Nyquist criterion [4]:

$$-F_D(M)G(j\omega) + 1 = 0 \tag{28}$$

the phase condition of the limit cycle is equal to:

$$\angle F_D(M)G(j\omega) = 0^\circ \tag{29}$$

while the magnitude condition of the limit cycle is equal to:

$$|F_D(M)G(j\omega)| \quad = 1 \tag{30}$$

Since the phase of $F_D(M)$ is equal to 0°, the angular oscillation frequency is thus obtained by using Eq. (29) and finding the frequency at which the phase of $G(j\omega)$ is equal to 0°:

$$\omega = \frac{1}{\sqrt{LC}} \tag{31}$$

while the single-ended oscillation amplitude M is obtained by substituting Eq. (31) into Eq. (30):

$$\frac{2I_{BIAS}}{\pi M}\frac{R}{2} = 1 \tag{32}$$

such that

$$M = \frac{I_{BIAS}R}{\pi} \tag{33}$$

To confirm the validity of this analysis, a differential negative resistance oscillator with an oscillation frequency of around 1.59 GHz, a biasing current I_{BIAS} of 1 mA and a supply voltage V_{DD} of 2.5 V was designed and is shown in **Figure 9**. The NMOS transistors used in the design have a transconductance parameter k_n of $120\mu A/V^2$ and a threshold voltage v_{tn} of 0.6 V. The current mirror biasing transistors M_3 and M_4 have an aspect ratio (W/L) of 25 to achieve an overdrive voltage $(V_{GS} - v_{tn})$ of 0.8165 V, where W is the gate width and L is the gate length of the transistors. The differential pair M_1 and M_2 were designed with an aspect ratio of 200 to achieve a transductance g_m of 4.8 mS and an overdrive voltage of around 0.2 V at a d.c. current of 0.5 mA. As per Eq. (31), the LC tank has a total inductance L of 2 nH and a total capacitance C of 5 pF.

Transient simulations were obtained for the designed oscillator using a generic SPICE simulator for various values of R, which is the total equivalent loss of the LC

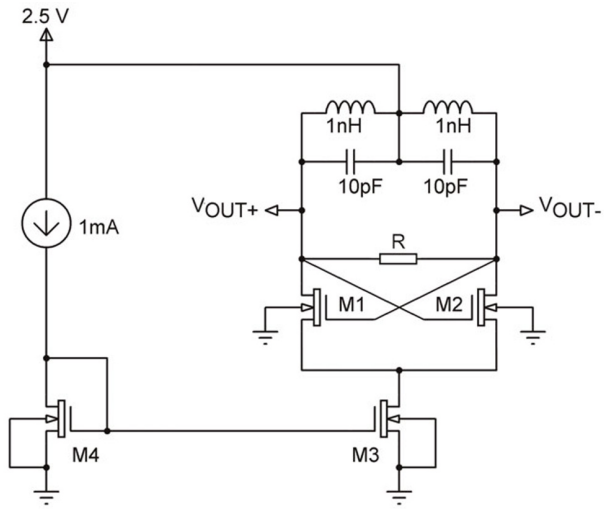

Figure 9.
Schematic diagram of the 1.59 GHz differential negative resistance oscillator.

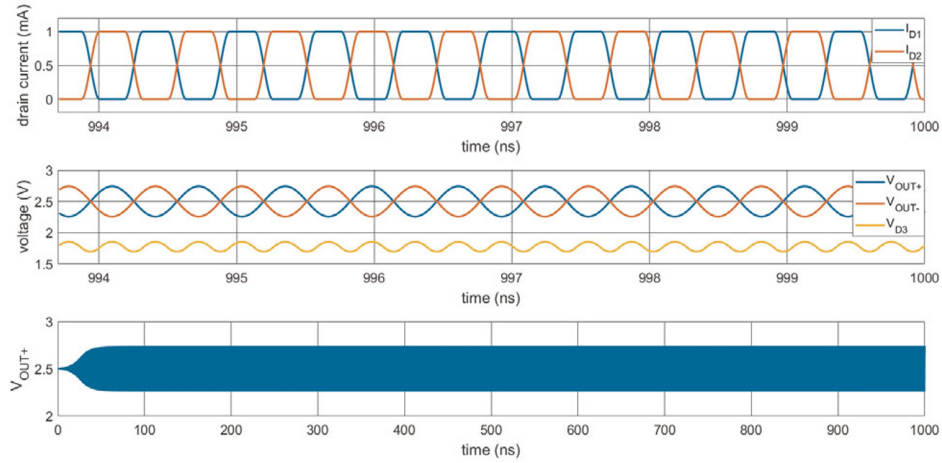

Figure 10.
Transient simulation results of the designed differential negative resistance oscillator with an LC tank loss of 800 Ω *obtained using a generic SPICE simulator.*

tank circuit and mainly depends on the quality factor of the inductor and the capacitor. **Figure 10** shows the steady-state transient simulation results obtained with $R = 800\ \Omega$.

An oscillation amplitude M of 0.243 V over a d.c. voltage of 2.5 V and an oscillation frequency of 1.585 GHz were achieved. **Figure 10** shows the transient plots of the drain currents (I_{D1} and I_{D2}) of transistors M_1 and M_2, the differential voltage outputs V_{OUT+} and V_{OUT-}, the common mode drain voltage of transistor M_3 (V_{D3}) and the oscillation transient built-up. The oscillation amplitude M obtained in the simulation is close to the value predicted by Eq. (33), which is equal to 0.255 V. The discrepancy of around 5% can be attributed to the fact that while the transconductance g_m of transistors M_1 and M_2 is large enough to provide sustained oscillations, it is not infinite and thus, the drain current waveforms are not ideal square waves as assumed in obtaining Eq. (26).

Figure 11 shows a graph that compares the simulated oscillation amplitude with the estimated value given by Eq. (33) for various values of R. For oscillation amplitude

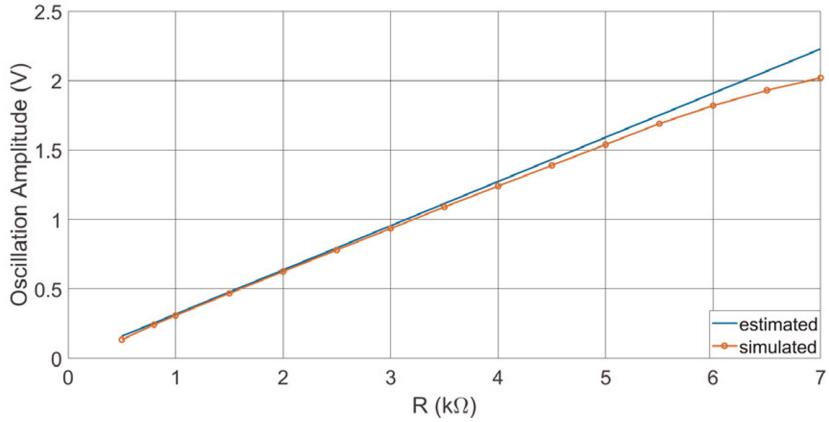

Figure 11.
Comparison of the estimated and simulated oscillation amplitude values for various values of R.

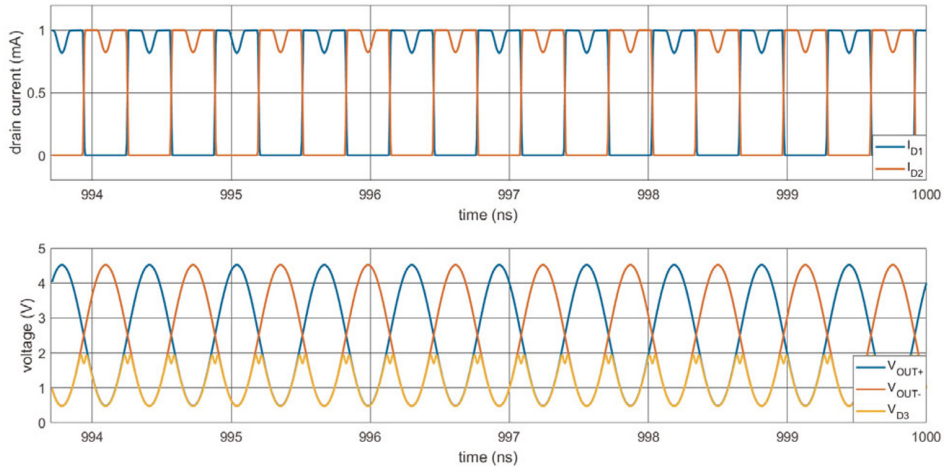

Figure 12.
Transient simulation of the differential negative resistance oscillator with an LC tank loss of 7 kΩ.

values less than 0.935 V (which is equivalent to a R value of 3 $k\Omega$), transistor M_3 always operates in the pinch-off region since its drain-to-source voltage is higher than its overdrive voltage (0.8165 V) and thus, the biasing current I_{BIAS} provided to the cross-coupled differential pair remains constant throughout the oscillation cycle and close to 1 mA.

When M is much greater than 0.935 V, unwanted distortion is introduced as can be noticed from the waveforms of I_{D1}, I_{D2} and V_{D3} in **Figure 12**, since transistor M_3 would not be operating in the pinch-off region during the whole oscillation cycle and a dip is noticed in the biasing current. **Figure 12** presents the transient simulation of the oscillator for R = 7 $k\Omega$. For the given transistor parameters and a d.c. drain current of 0.5 mA, the gate-to-source d.c. voltage of transistor M_1 (V_{GS1}) or M_2 (V_{GS2}) is equal to 0.8 V and the overdrive voltage of transistor M_3 is around 0.8165 V. Thus, if the gate voltage of transistor M_1 (V_{G1}) or M_2 (V_{G2}) is less than 1.6165 V ($V_{DD} - M = 1.565\ V$ where $M = 0.935\ V$), the values provided by Eq. (33) start to become inaccurate. Nonetheless, one would never operate this oscillator beyond this amplitude due to an increase in the total harmonic distortion and AM-to-PM noise upconversion.

4.2 Colpitts oscillator

The Colpitts oscillator is another type of LC tank oscillator that uses a combination of inductors and capacitors to generate a stable sinusoidal output [23]. At its core, it relies on a resonant tank circuit and positive feedback to maintain oscillations without an external input. The circuit's defining feature is the capacitive voltage divider formed by two series capacitors in parallel with an inductor, as shown in **Figure 13**. This arrangement allows a portion of the output signal to be fed back in the correct phase to sustain oscillations. Because of the split-capacitor design, the Colpitts oscillator tends to demonstrate better stability and reduced harmonic distortion compared to alternative oscillators. In transistor-based implementations, one bipolar junction transistor (BJT) or field-effect transistor (FET) is used to amplify the feedback signal and compensate for losses.

Figure 14 shows the equivalent circuit of the LC resonator tank of a Colpitts oscillator where R is the equivalent loss of the tank, L is the inductance and R' is the input resistance seen at the source of the MOS transistor, while C_1 and C_2 form the capacitive divider across the output v_{OUT}. The capacitive divider ratio is given by Eq. (34):

$$\frac{v_F}{v_{OUT}} = \frac{j\omega C_1 R'}{j\omega(C_1 + C_2)R' + 1} \tag{34}$$

which can be approximated by Eq. (35):

$$\frac{v_F}{v_{OUT}} = n = \frac{C_1}{C_1 + C_2} \tag{35}$$

for a high resonant frequency ω. The equivalent admittance of the LC resonator tank can be expressed as Eq. (36):

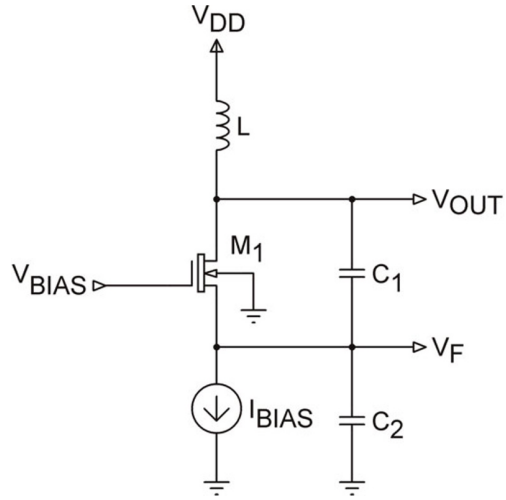

Figure 13.
NMOS-based common-gate Colpitts oscillator (with simplified biasing).

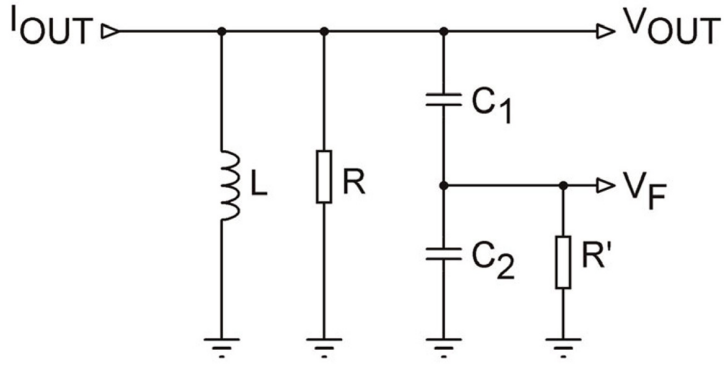

Figure 14.
Equivalent circuit of the LC resonator tank of a Colpitts oscillator.

$$\frac{1}{G(j\omega)} = \frac{i_{OUT}}{v_{OUT}} = j\omega n C_2 + \frac{1}{j\omega L} + \frac{1}{R} + \frac{n^2}{R'} \tag{36}$$

The Colpitts oscillator can be represented using the non-linear closed-loop model given in **Figure 15**, which consists of a non-linear active element, an inversion unity gain that models the inverting nature of the active device, a feedback gain n given by Eq. (35) and an LC tank passive equivalent linear element circuit defined by Eq. (36), where $C_{EQ} = \frac{C_1 C_2}{C_1 + C_2}$ is the equivalent capacitance, L is the inductance and $R_{EQ} = \frac{RR'}{R' + Rn^2}$ is the loaded equivalent loss of the tank circuit, where R' is equal to

$$R' = \frac{1}{g_m} \tag{37}$$

where g_m is the small-signal transconductance of the MOS transistor M_1. **Figure 16** shows the input and output waveforms for the peak detector non-linear element, which is formed by the transistor M_1, which is biased by the current source I_{BIAS}, and the equivalent capacitance C_{EQ}. Close to the negative peak of the output sinusoid v_{OUT}, M_1 injects a current spike of width t_1 and amplitude I_p, which sustains the oscillations.

Using Eq. (2) with $k = 0$, I_{BIAS} can be expressed in terms of I_P:

$$I_{BIAS} = \frac{A_0}{2} = \frac{1}{2\pi}\int_0^{\omega t_1} I_p \, d\omega t = \frac{I_P t_1}{T} \tag{38}$$

where T is the oscillation periodic time, while using Eq. (2) with $k = 1$,

$$A_1 = \frac{1}{\pi}\int_0^{\omega t_1} I_p \cos(\omega t) d\omega t = \frac{I_P \sin(\omega t_1)}{\pi} \tag{39}$$

Using Eq. (3) with $k = 1$, gives

$$B_1 = \frac{1}{\pi}\int_0^{\omega t_1} I_p \sin(\omega t) d\omega t = \frac{I_P \ (1 - \ cos \ (\omega t_1))}{\pi} \tag{40}$$

If t_1 is very small (i_{OUT} is ideally a Fermi-Dirac impulse), then A_1 can be expressed as Eq. (41) by using Eq. (38):

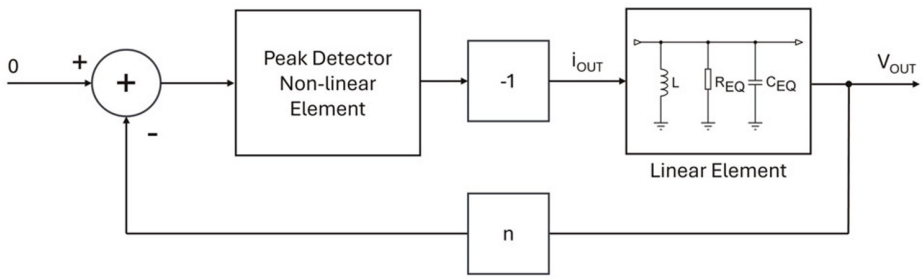

Figure 15.
Non-linear closed-loop model of the Colpitts oscillator.

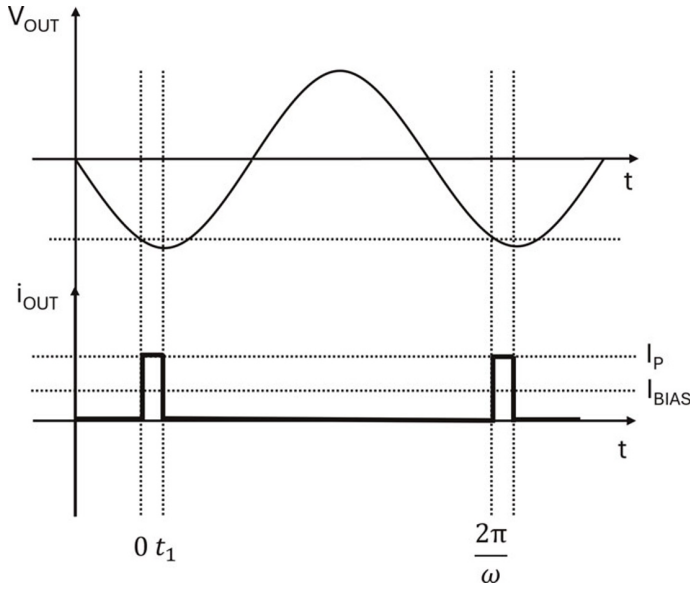

Figure 16.
Input and output waveforms for the peak detector non-linear element.

$$A_1 = \frac{2I_P t_1}{T} \approx 2I_{BIAS} \tag{41}$$

and B_1 is approximately equal to zero. This means that the describing function $F_D(M)$ for the non-linear element in this oscillator can be defined as:

$$F_D(M) = \frac{i_{OUT}}{-v_F} \approx \frac{2I_{BIAS}}{nM} \angle 0^\circ \tag{42}$$

where M is the oscillation amplitude. Since the phase of $F_D(M)$ is equal to 0°, the angular oscillation frequency is thus obtained by using Eq. (29) and finding the frequency at which the phase of $G(j\omega)$ is equal to 0°:

$$\omega = \frac{1}{\sqrt{L\left(\frac{C_1 C_2}{C_1 + C_2}\right)}} \tag{43}$$

while the oscillation amplitude M is obtained by substituting Eq. (43) into Eq. (30) and using Eqs. (36) and (42):

$$\frac{2I_{BIAS}}{nM} nR_{EQ} \approx 1 \tag{44}$$

such that

$$M \approx 2I_{BIAS} R_{EQ} \tag{45}$$

To check the validity of this analysis, a common gate Colpitts oscillator with an oscillation frequency of around 60 MHz, a biasing current I_{BIAS} of 1 mA and a supply

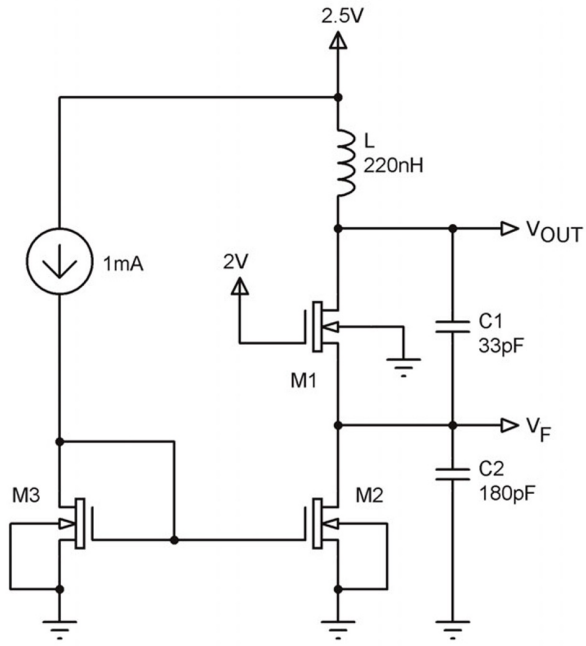

Figure 17.
Schematic diagram of the 60 MHz NMOS based common gate Colpitts oscillator.

voltage V_{DD} of 2.5 V was designed and simulated using SPICE. Its schematic diagram is shown in **Figure 17**. The NMOS transistors used in the design have a transconductance parameter k_n of 120$\mu A/V^2$ and a threshold voltage v_{tn} of 0.6 V.

For the particular component values shown, the capacitive divider factor n is estimated to be 0.155 using Eq. (35). Transistor M_1 is biased with a gate voltage V_{G1} of 2 V and overdrive voltage of around 0.2 V at a 1 mA biasing current. The transconductance g_m is thus equal to 9.8 mS such that at resonance, the loaded equivalent loss of the tank circuit R_{EQ} is equal to 708 Ω for R equal to 850 Ω. The absolute minimum acceptable transconductance $g_{m(min)}$ for sustained oscillations is given by Eq. (46) [23] and works out to 8.98 mS:

$$g_{m(min)} \geq \frac{1}{R(n-n^2)} \tag{46}$$

Using Eq. (45), the oscillation amplitude is estimated to be equal to 1.42 V. The SPICE simulation results of the designed oscillator are shown in **Figure 18**, indicating oscillation amplitude of 1.39 V. Eq. (45) is an approximate equation since in the analysis the capacitive divider was treated as an ideal transformer and i_{OUT} was taken to be an ideal Fermi-Dirac impulse. From **Figure 18** one may note that the drain current I_{D1} of transistor M_1 is almost sinusoidal since its g_m is not much larger than the $g_{m(min)}$.

5. Automatic amplitude control and AM-to-PM noise minimization

The DFM discussed in the previous sections provides important insights into the behaviour of oscillators. For the two practical RF oscillators presented and analysed in

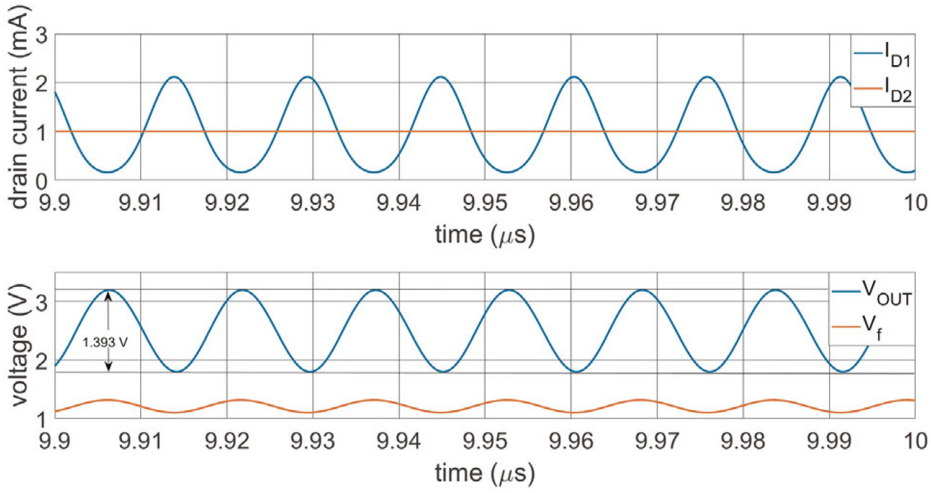

Figure 18.
Transient simulation results of the designed 60 MHz Colpitts oscillator.

Section 4, the DFM shows that they exhibit oscillation amplitude that is independent of the initial conditions present upon powering the circuitry. This is provided through the non-linear active devices used to sustain the oscillations. The DFM models the non-linear active devices by a linearised transfer function $F_D(M)$ as shown by Eqs. (26) and (42). If initially, the oscillation amplitude is small, then $F_D(M)$ is large such that a large current is injected in the LC resonator tank causing the oscillation amplitude to increase since $F_D(M)$ is inversely proportional to M. Eventually, the oscillation amplitude reaches a steady-state value since the effective transconductance $g_{m(eff)}$ of the active devices is reduced to precisely compensate for the loss in the LC resonator tank. For instance, **Figure 19** shows the transient simulation of a differential negative resistance oscillator with $L = 1\,nH$, $C = 1\,pF$, $R = 1\,k\Omega$ and an I_{BIAS} of 2 mA (refer to **Figure 6**). The oscillator exhibits steady-state oscillation amplitude of 0.637 V as per Eq. (33) and an oscillation frequency of 5 GHz as per Eq. (31). While **Figure 19** shows the oscillation build-up, it also shows the transient variation of the effective transconductance $g_{m(eff)}$ given by $|F_D(M)|$, which reaches a steady-state value equal to around $2\,mS$, providing an open loop gain of unity at the oscillation frequency as per Eq. (30). In fact, the minimum effective transconductance for such oscillator to achieve sustained oscillations given by Eq. (47) [23] confirms this result for R = $1\,k\Omega$.

$$g_{m(eff)} = \frac{2}{R} \tag{47}$$

Eqs. (33) and (45) show that the steady-state value of the oscillation amplitude depends on both the biasing current and the equivalent dynamic resistance of the LC resonator tank. Since this dynamic resistance is a function of frequency, one expects a variation of the oscillation amplitude across the frequency tuning range of the oscillator. Eqs. (33) and (45) highlight the importance of including an automatic amplitude control (AAC) mechanism in an RF oscillator circuit, particularly to one that is designed to provide a wide frequency tuning range [25]. AAC guarantees a reliable oscillator start-up by requiring only a small excess loop gain. This, in turn, helps

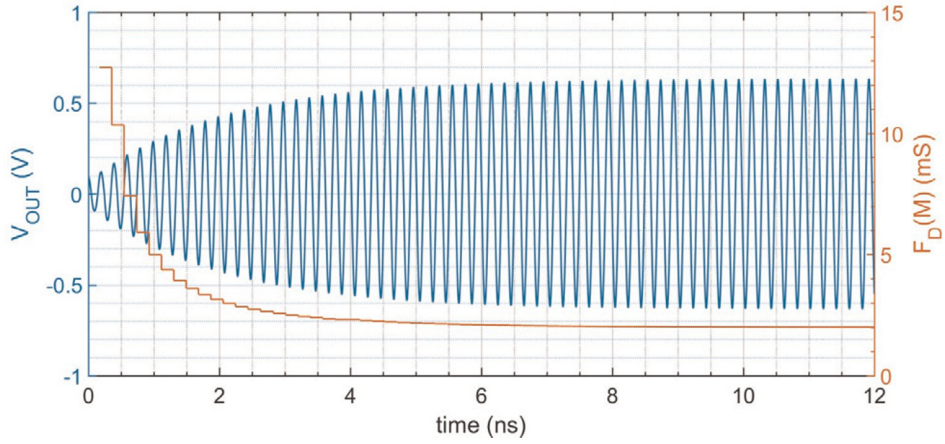

Figure 19.
Transient simulation of a differential negative resistance oscillator.

remove unwanted harmonics from the output and reduces steady-state power consumption thanks to smaller transistor sizes. Moreover, it ensures a constant output power regardless of variations in the resonator quality factor, temperature or process. This is especially crucial for designing the stages that follow the oscillator in frequency synthesiser architectures, as well as for circuits like mixers connected to the oscillator output. Furthermore, it enables setting an optimal bias point to achieve low phase noise [25]. The oscillation amplitude is ideally kept constant over the whole tuning range by varying the biasing current I_{BIAS} so that non-linear effects, such as the modulation of the parasitic and varactor capacitances, which lead to noise upconversion, are minimised [26]. For instance, in the differential negative resistance oscillator discussed in **Section 4.1**, the AM-to-PM conversion of flicker noise from both the biasing (M_3) and negative resistance transistors (M_1 and M_2) can also take place due to the AM-to-PM transfer function exhibited by the cross-coupled transistors [26]. This up-conversion factor depends on both the harmonic distortion at the output nodes and the biasing of the cross-coupled transistor [25, 26].

6. Conclusions and future work

This chapter explored the application of describing functions in predicting the behaviour of non-linear oscillators. It delved into the theoretical foundations of describing functions and their practical use in predicting limit cycles in oscillators, highlighting their ability to estimate the oscillation amplitude and frequency. Through analytical derivations and case studies of some oscillators, this work demonstrated how describing functions bridge the gap between rigorous non-linear analysis and practical engineering approximations. The limitations, accuracy considerations and alternative techniques were also discussed, providing a comprehensive understanding of when and how to effectively use describing functions in oscillator analysis and design. The discussion was supported by a literature survey on the use of describing functions in oscillator design and analysis and its relevance to automatic amplitude control mechanisms and the minimisation of AM-to-PM noise conversion. The

following is some future work that one could pursue to advance the field of predicting the behaviour of electronic oscillators using DFM. While some of these may have seen limited consideration in the literature, they remain relatively unexplored or open-ended in terms of achieving comprehensive solutions.

Standard DFM typically use a single-tone sinusoidal input to derive the first harmonic approximation. However, many practical oscillators exhibit higher harmonics, intermodulation products or multi-tone signals in their non-linear operation. Extending DFM to capture multi-frequency inputs or higher-order harmonic content could offer more accurate predictions of phenomena such as distortion, harmonic locking and sub-harmonic or super-harmonic oscillations. Chaos, quasi-periodicity or multi-limit-cycle phenomena can also arise in strongly non-linear circuits. Traditional DFM are aimed primarily at stable limit cycles. Extending DF analyses to detect the onset of chaos or identify quasi-periodic attractors, potentially by examining sub- and super-harmonic components or analysing multiple limit cycles, is an interesting research avenue.

Practical oscillator implementations have time-varying parameters such as temperature-dependent transistor parameters, ageing or bias circuit drift. Describing functions often rely on the assumption of a time-invariant non-linearity. Adapting the DFM theory to time-varying behaviours, such as piecewise or slowly varying modelling, to study how oscillator characteristics evolve is another relevant research question. This might incorporate periodic re-linearisation or perturbation-based techniques. Oscillator performance in practical applications is significantly affected by noise, which degrades phase noise. Traditional describing function-based methods ignore or only marginally address noise. One may formulate a stochastic describing function methodology that captures the interplay between non-linearities and noise sources, potentially coupling DF analyses with the statistical methods or stochastic differential equations.

Multiple oscillators may be coupled together, such as injection-locked oscillators [27], quadrature output oscillators [28] or multi-phase oscillator arrays [29]. Linear or single-device DF analyses may fail to account for coupling. It would be interesting to develop network-level DFM where each oscillator or stage is represented by a describing function, and the interactions among these blocks are modelled to predict collective phenomena like synchronisation, injection locking, mode hopping and pattern formation. By pursuing these directions, one can expand the DFM and apply it to a wider range of practical oscillators, from low-frequency relaxation circuits to high-frequency RF or mm-wave designs, while incorporating emerging complexities such as multi-tone signals, stochastic noise and intricate coupling between multiple non-linear elements.

Dedication

I dedicate this book chapter to my beloved son, Harry, who will always be in my thoughts. May this note bring him solace and happiness, knowing that his mother, Charmaine, and I have loved him as our own child from the moment our paths crossed and eagerly awaited the day he would be in our arms.

Author details

Owen Casha
Department of Microelectronics and Nanoelectronics, University of Malta, Msida, Malta

*Address all correspondence to: owen.casha@um.edu.mt

References

[1] Casha O, Grech I, Micallef J. Issues on the design and implementation of radio frequency CMOS LC tank voltage-controlled oscillators. Journal of Analog Integrated Circuits and Signal Processing. 2009;**61**(2):159-170

[2] Pepe F, Bonfanti A, Levantino A, Samori C, Lacaita AL. A wideband voltage-biased LC oscillator with reduced flicker noise up-conversion. In: Proceedings of the 2013 IEEE Radio Frequency Integrated Circuits Symposium; 2–4 June 2013; Seattle, WA, USA. USA: IEEE; 2013. pp. 27-30

[3] Raab B, Kaufmann M, Rauchenecker M, Ostermann T. Robust and efficient design plan for integrated differential negative-gm LC VCOs. In: Proceedings of the 22nd International Conference Mixed Design of Integrated Circuits and Systems; 25–27 June 2015; Torun, Poland. USA: IEEE; 2015. pp. 386-389

[4] Modern OK. Engineering C. 5th edition. London, UK: Pearson; 2021

[5] Krack M, Gross J. Harmonic Balance for Nonlinear Vibration Problems. Switzerland: Springer Cham; 2019

[6] Allgower EL, Georg K. Numerical Continuation Methods - an Introduction. Heidelberg: Springer Berlin; 1990

[7] Krylov N, Bogolyubov N. Introduction to Nonlinear Mechanics. New Jersey, USA: Princeton University Press; 1947

[8] Kochenburger RJ. A frequency response method for analyzing and synthesizing contactor servomechanisms. Transactions of the American Institute of Electrical Engineers. 1950;**69**(1):270-284

[9] Bissell CAA. Andronov and the development of soviet control Engineering. IEEE Control Systems Magazine. 1998;**18**(1):56-62

[10] Pranayanuntana P, Anuntahirunrat K, Fongsamut C, Kaewsaiha P. The describing function method and the analysis of the magnitude stabilization phenomenon in a nonlinear oscillators. In: Proceedings of IEEE International Symposium on Communications and Information Technology; 12–14 October 2005; Beijing, China. USA: IEEE; 2005. pp. 420-423

[11] Rodríguez-Vázquez A, Leñero-Bardallo JA. When Barkhausen's criterion does not suffice and you must rely on the forgotten art of oscillator design. In: Proceedings of the 2024 XVI Congreso de Tecnología, Aprendizaje y Enseñanza de la Electrónica (TAEE); 26–28 June 2024; Malaga, Spain. USA: IEEE; 2024. pp. 1-6

[12] Meszaros G, Ladvanszky J, Berceli T. Oscillator design using two-port describing functions. In: Proceedings of IEEE International Conference on Computer Communications; 10–15 April 2016. San Francisco, CA, USA. USA: IEEE; 2016. pp. 1-9

[13] Reich HJ. Describing-function analysis of thermally self-excited mechanical oscillators. IEEE Transactions on Education. 1968;**11**(2): 116-119

[14] Vidal E, Poveda A, Ismail M. Describing functions and oscillators. IEEE Circuits and Devices Magazine. 2001;**17**(6):7-11

[15] Wang T. Analyzing oscillators using describing functions. arXiv: 1710.02000. 2017:1-19

[16] Stork M. Voltage controlled oscillators: Sinusoidal and square wave ring and relaxation oscillators. In: Proceedings of the 3rd Mediterranean Conference on Embedded Computing; 15–19 June 2014; Budva, Montenegro. USA: IEEE; 2014. pp. 180-183

[17] Jahangir MZ, Paidimarry CS. Design of a Novel Charge Pump based current starved ring oscillator with reduced phase noise. In: Proceedings of the 2023 International Conference for Advancement in Technology; 24–26 January 2023; Goa, India. USA: IEEE; 2023. pp. 1-3

[18] Eijk LF, Kostić D, Khosravi M, Hosseinia SH. Higher order sinusoidal-input describing function analysis for a class of multiple-input multiple-output convergent systems. IEEE Transactions on Automatic Control. 2025;**70**(1): 673-680

[19] Chen D, Wang Y, Chen X, Huang W, Xie J. Duffing nonlinearity localization via extension energy confinement in an elastic mode semicircular beams resonator. IEEE Electron Device Letters. 2019;**40**(2): 314-317

[20] Sung S, Chang BS, Lee KY, Lee YJ. A vibration-controlled resonant accelerometer design and its application to the single structured gyroscope/ accelerometer system. In: Proceedings of the 2007 IEEE International Conference on Vehicular Electronics and Safety; 13–15 December 2007; Beijing, China. USA: IEEE; 2007. pp. 1-6

[21] Mouro J, Pinto R, Paoletti P, Tiribilli B. Microcantilever: Dynamical response for mass sensing and fluid characterization. Sensors (Basel). 2020; **21**(1):115

[22] Pinto AM, Souza RRN, Solano JEV, Lima ER, Manera LT. LC-VCO design with switched Varactor Array for L-band in 65 nm CMOS technology. In: Proceedings of the 2024 IEEE International Conference on Design, Test and Technology of Integrated Systems; 14–16 October 2024; Aix-EN-PROVENCE, France. USA: IEEE; 2024. pp. 1-6

[23] Lee TH. The Design of CMOS Radio-Frequency Integrated Circuits. 2nd ed. UK: Cambridge University Press; 2003

[24] Chaichana A, Mhuenpong K, Sotner R, Jaikla W. Electronically controllable Colpitts oscillator with amplitude controllability using commercially available ICs. In: Proceedings of the 13th International Conference on Power, Energy and Electrical Engineering; 25–27 February 2023; Tokyo, Japan. USA: IEEE; 2023. pp. 22-26

[25] Casha O, Grech I, Micallef J, Gatt E. Design of a 1.2 V low phase noise 1.6 GHz CMOS buffered quadrature output VCO with automatic amplitude control. In: Proceedings of the 13th IEEE International Conference on Electronics, Circuits and Systems; 10–13 December 2006; Nice, France. USA: IEEE; 2006. pp. 192-195

[26] Casha O, Grech I, Micallef J, Gatt E. Design considerations and device selection in the implementation of low phase noise LC-VCOs. In: Proceedings of the 14th IEEE International Conference on Electronics, Circuits and Systems; 11–14 December 2007; Marrakech, Morocco. USA: IEEE; 2007. pp. 1083-1086

[27] Xin K. Frequency domain modeling and performance analysis of injection-locked LC oscillator. IEEE Transactions on Circuits and Systems II: Express Briefs. 2024;**71**(1):11-15

[28] Kadam M, Kudabay Y, Oliveira P, Wohlmuth HD. Issakov V. A low phase noise 12 GHz LO generation with quadrature outputs in 0.13 μm SiGe BiCMOS. In: Proceedings of the 15th German Microwave Conference; 11–13 March 2024; Duisburg, Germany. USA: IEEE; 2024. pp. 93-96

[29] Dutta S, Ranjan R, Kumari P, Sinha P, Ranjan RK, Singh DK. Operational Transconductance amplifier (OTA) based dual mode multiphase oscillator. In: Proceedings of the 5th International Conference on Recent Trends in Computer Science and Technology; 9–10 April 2024; Jamshedpur, India. USA: IEEE; 2024. pp. 332-337